Journal of Coastal Research	31	6	1363–1374	Coconut Creek, Florida	November 2015

Marine Currents in the Gulf of Urabá, Colombian Caribbean Sea

Carlos A. Escobar*, Liliana Velásquez, and Federico Posada

Department of Civil Engineering
Universidad EAFIT
Medellín, Antioquia, Colombia

www.cerf-jcr.org

www.JCRonline.org

ABSTRACT

Escobar, C.A.; Velásquez, L., and Posada, F., 2015. Marine currents in the Gulf of Urabá, Colombian Caribbean Sea. *Journal of Coastal Research,* 31(6), 1363–1374. Coconut Creek (Florida), ISSN 0749-0208.

A comprehensive study of the marine currents of the Gulf of Urabá is presented for temporal scales ranging from intertidal to seasonal. The analyses made were based on three-dimensional (3D) numerical modeling and extensive current observations. The hydrodynamic model based on the Delft3D platform included the influence of different forcings such as tide, waves, atmosphere, river discharges, and density gradients. Because field data concerning these variables are scarce for the study area, measuring campaigns, in combination with global models and databases, were used to overcome this condition. The evaluation of the model was attained by the use of unprecedented field data obtained in different climatic seasons through a mobile gauge station. This station registered instantaneous vertical profiles of flow along 1200 km with approximately 50-m spacing. This type of measurement was preferred instead of those obtained from stationary stations, because the spatial gradients of the currents were much greater than their temporal variations. The good agreement of the 3D mathematical model in the reproduction of the observed instantaneous currents supported its use in defining the marine currents in the gulf. A combined analysis of the model results and the measured currents revealed a complex circulation pattern comprising simultaneously typical estuarine circulation, one- to three-layer flows, and even inverse circulation. This flow complexity would hardly have been determined through common measurement methodologies based on stationary gauge stations.

ADDITIONAL INDEX WORDS: *Estuarine dynamics, salinity stratification, hydrodynamic model, current measurement.*

INTRODUCTION

The geostrategic location of the Gulf of Urabá has historically represented an opportunity for Colombia to connect the Caribbean Sea with the Pacific Ocean through an interoceanic canal (Henao and Correa, 2007; Hubach, 1930; Melman, 2011; Post, 2011; Trautwine, 1854). This is an initiative that has commonly been included in government plans and has persisted as an aspiration to the present day, as has the construction of a strategic port that would serve the markets of the Caribbean, North American Free Trade Agreement (NAFTA) countries, Europe, and the Pacific Basin (BIRD, 2010). The realization of these projects would make the gulf fundamental for Colombia within the scope of globalized markets. As a result, issues like navigation, design of marine infrastructure, coastal evolution, and conservation of marine ecosystems would become relevant and urgent matters when considering the predicted magnitude of short- and medium-term investment opportunities. An adequate study of these issues requires reliable information about the hydrodynamics of the gulf. Such information is equally valuable in the understanding and exploration of possible solutions to the current problems of erosion (Correa and Vernette, 2004), sedimentation (Díaz, 2007), water quality (Lonin and Vasquez, 2005), and reduction of live coral cover (Díaz, Díaz, and Sánchez, 2000) that the region confronts.

Since the 1990s, a number of investigations have focused on determining circulation patterns in the Gulf of Urabá. Among them, analyses of satellite images were used to establish surface currents (Chevillot *et al*., 1993; Molina, Molina, and Chevillot, 1992). Subsequently, because of the advance in computational techniques, hydrodynamic three-dimensional (3D) models were implemented to describe the gulf circulation. These models were based on the Estuary, Lake and Coastal Ocean Model and the Estuarine, Coastal and Ocean Modeling System with Sediments modeling systems (wave influence was neglected), which provided additional information about subsurface currents and circulation patterns (Lonin and Vasquez, 2005; Montoya, 2010; Roldán, 2008).

However, the lack of measurements of marine currents and discharges of the Atrato River (key hydrodynamic forcing) restricted the previous prediction of these variables to indirect model approaches based on thermohaline observations. Thus, our main goal was the determination of circulation patterns in the Gulf of Urabá (a tropical region where an estuary and a "bird foot" delta systems converge) based on both field measurements and numerical modeling. This purpose is of particular interest because most similar studies have been developed in midlatitudes, with lower freshwater input to the oceans, higher Coriolis force, and higher recognition of their practical importance in respect to the tropics (Simpson, 1997).

A 3D hydrodynamic model was calibrated and validated to provide a wider and finer temporal and spatial coverage of the

DOI: 10.2112/JCOASTRES-D-14-00186.1 received 23 September 2014; accepted in revision 24 January 2015; corrected proofs received 10 March 2015; published pre-print online 7 April 2015.
*Corresponding author: carloses@eafit.edu.co

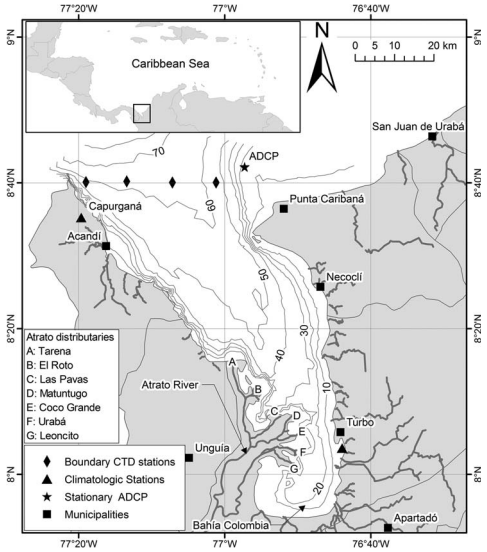

Figure 1. Study area, measurement stations, and bathymetric data (in meters) from the nautical chart developed by the Dirección General Maritima in 2009.

marine current information of the gulf, an expensive process if done exclusively using field measurements. The prediction capability of the model was quantified according to statistical parameters used for the evaluation of coastal models (Sutherland *et al*., 2004; Van Rijn, Grasmeijer, and Ruessink, 2000). The hydrodynamic model was applied to reproduce the currents during two climatic seasons (dry and rainy) and during a probable extreme event in the gulf (Chevillot *et al*., 1993; Osorio *et al*., 2010).

Study Area

The Gulf of Urabá is located in the southernmost region of the Caribbean Sea; it penetrates almost 80 km into the continent, with variable width ranging from 5.9 to 48.5 km (Figure 1). The dynamics of the gulf are fundamentally influenced by solid and liquid discharges from tributaries, winds, waves, tides, and density gradients (Escobar, 2011; Lonin and Vasquez, 2005; Montoya, 2010). The aforementioned factors significantly differ during the dry (December to April) and rainy (May to November) seasons, which occur in the area as a response of the latitudinal migration of the Intertropical Convergence Zone (Hastenrath, 1990).

The Gulf of Urabá receives a significant input of freshwater from various rivers—among them the Atrato River, draining one of the rainiest regions in the world. Taking into account the extent of its basin, the relative discharge of the Atrato is five to six times larger than that of the Amazon River (Poveda and Mesa, 1997). Such a discharge, along with the low energy of this marine system, causes high saline stratification in the gulf. Although the discharge of the Atrato River is of greatest relevance in the current circulation pattern in the gulf, it is one of the least monitored. Isolated measurements carried out near the mouths of this river in different climatic seasons showed discharges varying from 4138 to 5017 m^3/s.

The wind in the region has bimodal characteristics; during the dry season the NE trade winds are predominant, with an average speed of 3 to 4 m/s but intensifying in February up to 9.4 m/s (Chevillot *et al*., 1993). Because of the blocking action of these strong winds, the dry season is characterized by keeping larger volumes of freshwater in the gulf in respect to the rainy season (García, 2007), when winds from the S and SE predominate, with an average speed below 2 m/s (Roldán, 2008).

Waves in the Gulf of Urabá have not been fully studied, and *in situ* measurements are scarce. Based on global models such as Wavewatch III (Tolman, 1989), mean significant wave heights were estimated (at the northern boundary) to be around 0.75 and 1.5 m during the rainy and dry seasons, respectively. The gulf has a microtidal regime that is mixed semidiurnal with maximum amplitudes up to 40 cm in its narrower area (Correa and Vernette, 2004). Maximum tidal ranges observed at the northern boundary were slightly greater than 40 cm. This tidal range variation could be a consequence of the morphological constriction imposed by the delta of the Atrato River. Throughout the gulf, variations in water temperature and salinity of up to 4°C and 35, respectively, can be observed both horizontally and vertically.

METHODS

This section presents details about the measuring strategy (based mostly on mobile gauge stations) used to observe the marine currents in the Gulf of Urabá and the 3D numerical model implemented to predict them.

Measuring Campaigns

The influence of several external forcings in the gulf's flow and the absence of a unique predominant force result in higher complexity and spatial variability of its currents. Different processes govern the hydrodynamics in certain regions; that is, river advection predominates near their mouths, tides become relevant in the gulf's narrower area, and wave effects are more significant at the north boundary and in nearshore areas while saline stratification dominates in the central and southern areas of the gulf (Escobar, 2011; Montoya, 2010).

These conditions, in combination with the microtidal regime, make the currents' temporal gradients smaller than their spatial ones. Therefore, field campaigns were designed emphasizing the observation of the spatial variability of the currents. To accomplish such a goal, a mobile gauge station was used. This method renders a considerable amount of spatially distributed information; however, it requires more human effort and time in comparison with autonomous stationary gauges.

Figure 2 presents the locations of current measurements along transects corresponding to the dry (April 2010), transition (November–December 2011), and rainy (August 2009) seasons. The solid lines indicate a sole transect, while dotted lines mean multiple transects traversed during a tidal cycle. These cross-channel transects were planned to follow a regular pattern with separations between 3 to 5 km. However, a total spatial coverage of the gulf was not always possible because of weather conditions, logistical issues, or problematic data. The measurements were focused on the narrower area of the gulf

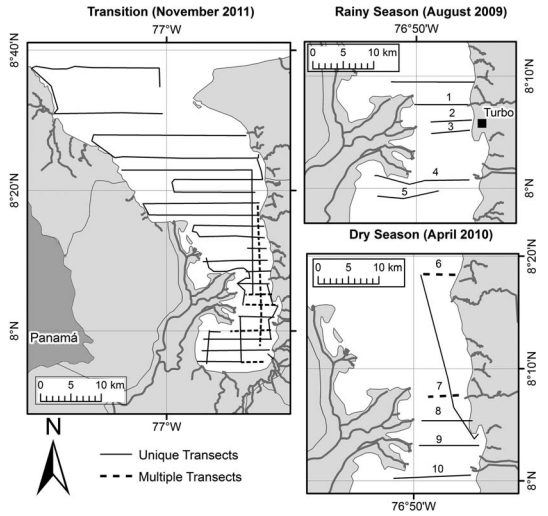

Figure 2. Locations of transects with currents' measurements.

where a more complex hydrodynamic condition was expected as a consequence of its vicinity to the Atrato's discharge, enhanced tidal currents, and flow stratification.

The transects indicated in Figure 2, with a total length of about 1200 km, were followed using vessels in which a broadband Workhorse Sentinel acoustic Doppler current profiler (ADCP) was pole mounted. The ADCP was operated with a frequency of 600 kHz and enabled the current profiles to be registered with a resolution of 1 m vertically and about 50 m horizontally. All current profiles were obtained after averaging 10 pings in a 15-s period. Quality control of the ADCP data was performed through the redundant measurement of the vertical velocity, available from the four-beam geometry of the instrument. In general, data with an error twice as high as the reported standard deviation of the horizontal velocity (given by the manufacturer under minimal ADCP motion) were removed from the dataset.

The temporal variability of the marine currents was taken into consideration through measurements carried out in the different climatic seasons of the gulf (Table 1). In addition, an upward-looking ADCP was deployed for a 3-month period. The mooring location of the ADCP at 18 m of depth (stationary gauge station) is indicated with a star in Figure 1. At this point, velocity profiles, tidal levels, and directional waves were continuously recorded from August to November 2010. All current profiles (ensembles) were obtained after averaging 46 pings every 20 minutes. Finally, in addition to current measurements, vertical profiles of temperature and salinity were registered in various stations scattered throughout the gulf (Table 1 and later Figure 6) using a conductivity temperature and depth (CTD) profiler.

Numerical Modeling

A 3D hydrodynamic model of the gulf was constructed based on the Delft3D modeling platform. This model includes the effects on the currents because of tides, waves, density gradients, wind drag, water discharges from the Atrato River,

Table 1. *Oceanographic surveys in the Gulf of Urabá.*

Date	Transects	Type
Aug. 28–31, 2009	64 km	Mobile station
Sep. 17–19, 2009	16 km	Mobile station
Apr. 6–16, 2010	105 km	Mobile station and CTD profiles
Aug. 15–Nov. 7, 2010	Punta Caribaná	Stationary station
Apr. 15–16, 2010	Atrato River	Mobile station
Nov. 6–11, 2010	Atrato River	Mobile station and CTD profiles
Nov. 18–Dec. 1, 2011	900 km	Mobile station and CTD profiles
Dec. 2–3, 2011	Atrato River	Mobile station

and several minor streams. The equational system and numerical solution used by Delft3D has been explained in length by various authors (Gerritsen *et al.*, 2007; Leendertse, 1967; Lesser *et al.*, 2004; Roelvink and Van Banning, 1994; Stelling and Leendertse, 1991; WL | Delft Hydraulics Staff, 2012); it is not repeated here in the interest of brevity. The κ-ε turbulence closure model (Rodi, 1980) was used to determine the vertical turbulent eddy viscosity and eddy diffusivity. The absolute flux, total solar radiation model was selected to define the heat fluxes across the sea surface (Octavio, Jirka, and Harleman, 1977).

The built-in interface between the Delft3D-FLOW module and the third-generation wave model Simulating Waves Nearshore (Booij, Ris, and Holthuijsen, 1999) was used to determine wave–current interaction. The latter allowed us to compute (1) wave-induced forces (Dingemans, Radder, and de Vriend, 1987), (2) wave-induced drift velocity (Stokes drift) because of the asymmetry of the orbital motion (Walstra and Roelvink, 2000), (3) wave-induced currents in the wave boundary layer "streaming" (Fredsöe and Deigaard, 1992), (4) wave-induced turbulence because of wave breaking and bottom friction (Walstra and Roelvink, 2000), and (5) enhancement of the bed shear stress by waves' and currents' nonlinear interaction (Fredsöe, 1984). These physical mechanisms reach great importance in defining nearshore currents and sediment transport, which are fundamental in coastal erosion studies required in the Gulf of Urabá.

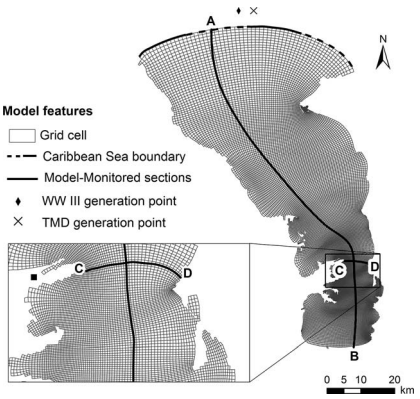

Figure 3. Curvilinear grid, model boundaries, and model-monitored sections.

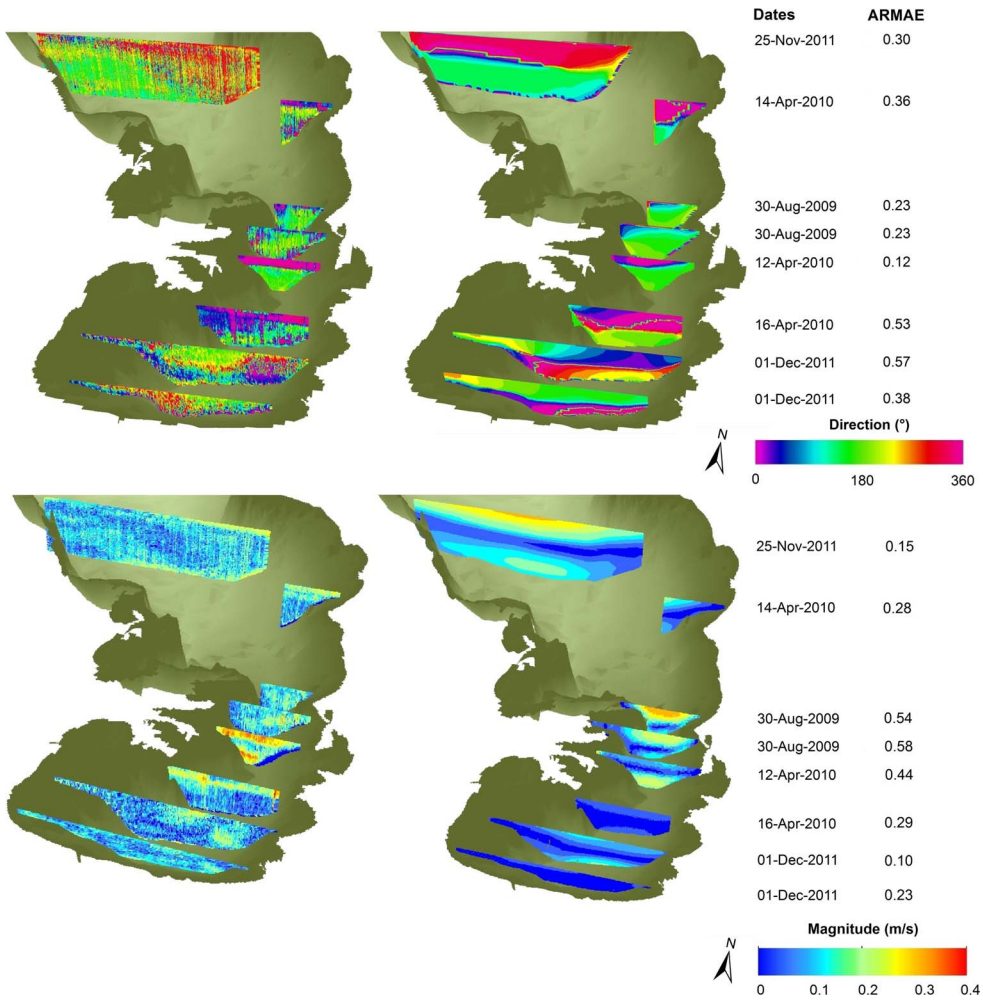

Figure 4. Currents in the Gulf of Urabá, (left) observed and (right) modeled. (Color for this figure is available in the online version of this paper.)

The hydrodynamic model solves its equational system in a horizontal curvilinear grid of approximately 22,000 cells exhibiting sizes ranging from 50 to 1200 m (Figure 3). The varying spatial resolution was established according to the coastal geometry and flow complexity of the gulf. The vertical dimension was discretized through 20 layers using a sigma coordinate system (Phillips, 1957). The upper, intermediate, and lower layers have thicknesses of 2.5, 5, and 7.5% of the total depth, respectively.

The external forces acting as boundary conditions for the model were obtained from several sources. Atmospheric data were gathered from climatological stations, such as Capurganá, Turbo, and Los Cedros (Figure 1). Information not provided by these stations was obtained from the National Centers for Environmental Prediction (NCEP) and the National Center for Atmospheric Research (NCAR) reanalysis (Kalnay *et al*., 1996) and North American Regional Reanalysis (NARR) (Mesinger *et al*., 2006) projects. The absence of tidal and wave gauges in the area led us to use the astronomical tide from a global tide model in the oceanic border, such as the Tide Model Driver (Egbert and Erofeeva, 2002). Wave characteristics in the northern boundary were defined through the results of the Wavewatch III model (Tolman, 1989). The discharges of minor tributaries into the gulf were obtained from hydrological balances (Velez, Poveda, and Mesa, 2000).

During three field surveys in April 2010, November 2010, and December 2011, the discharge of the Atrato River (the main tributary) and the thermohaline conditions were measured near the mouth of the main distributaries (Tables 1 and 2) and at the northern Boundary, respectively.

Model Calibration and Validation

The field data (Figure 2) was coupled with numerical modeling through the use of typical calibration and validation procedures. For calibration, transects of marine currents measured during the rainy season (August 2009) were used, whereas field observations carried out in the dry season were considered for validation (April 2010). Then, the model was "trained" to reproduce flow conditions during the rainy season (calm weather) and challenged to estimate the flow during the

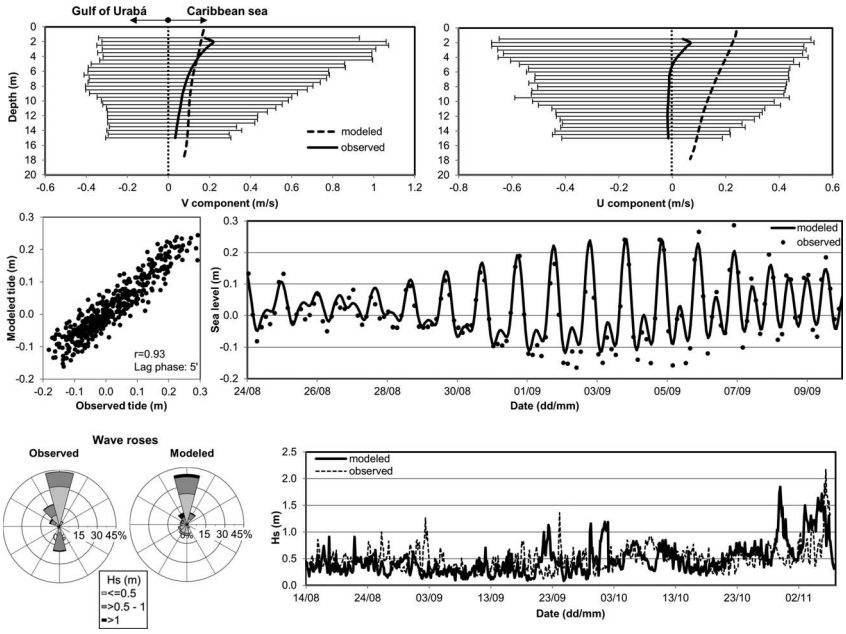

Figure 5. Sea conditions in the NE area of the Gulf of Urabá during the rainy season of 2010. (Top) Vertical profile of residual velocity and range of measured values, (left) north component and (right) east component; (middle) measured and modeled sea levels; and (bottom) measured and modeled significant wave heights.

"untrained" dry season, when the weather conditions are more severe. In case of success, a better chance to properly predict the hydrodynamics under "untrained" periods was assumed. The validation of the model was complemented with some additional tests performed through the comparison of the model predictions to other sets of measurements carried out by the stationary (August to November 2010) and mobile (transition period of November to December 2011) gauge stations.

By means of the calibration and sensitivity analysis procedures, the values for some unknown numerical and physical parameters were determined in the study area. The "one at a time" methodology described by Saltelli, Tarantola, and Campolongo (2000) allowed a separately modification of each parameter until a final model configuration generated the best fit between observations and modeled data; more details can be found in Velasquez (2013). Table 3 shows the estimated value of these parameters. For most of them, spatial and temporal variations were unknown and therefore were neglected in this model.

Later, the model performance was verified under a different climatic season to see whether these parameter values were still suitable. The discrepancies between observed and modeled currents in the dry season were statistically quantified through the mean absolute error (MAE), relative mean absolute error (RMAE) and average adjusted relative mean absolute error (ARMAE) parameters (Sutherland *et al.*, 2004; Van Rijn, Grasmeijer, and Ruessink, 2000):

$$\mathrm{MAE} = \langle |Y - X| \rangle \qquad (1)$$

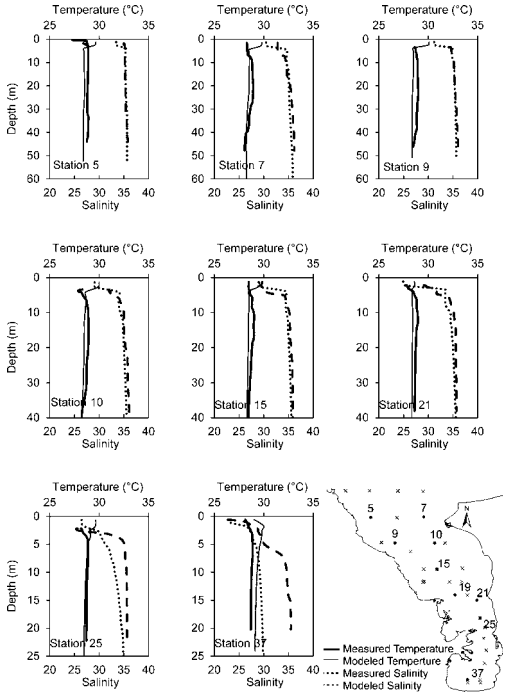

Figure 6. Modeled and observed temperature and salinity profiles in the Gulf of Urabá.

Table 2. *Flow discharges of the Atrato distributaries at three field campaigns.*

Distributary	$Q_{Apr.2010}$ (m^3/s)	$Q_{Nov.2010}$ (m^3/s)	$Q_{Dec.2011}$ (m^3/s)
El Roto	2849	2847	3201
Tarena	16.4	53.1	34.4
Matuntugo	484	547	754
Coco Grande	138	128	228
Urabá	7.4	11.6	11.6
Leoncito	628	860	777
Pavas	15.6	15.6	11.1
Total	4138	4462	5017

$$\mathrm{RMAE} = \frac{\langle |Y - X| \rangle}{\langle |S| \rangle} \tag{2}$$

$$\mathrm{ARMAE} = \frac{\langle |Y - X| - OE \rangle}{\langle |S| \rangle} \tag{3}$$

Here, X is the set of N observed values ($x_1,\ldots, x_N$); Y is the set of N modeled values ($y_1,\ldots, y_N$); OE is the observational error given by the ADCP position, averaging time, and weather conditions during the field survey; and

$$S = \left\{ \begin{array}{l} X, \text{ when } X \text{ correspond to current speed, or} \\ \text{Range of } X, \text{ when } X \text{ correspond to current direction} \end{array} \right\}.$$

Angular brackets denote average and vertical lines symbolize the modulus. In Equation (3), negative values of the numerator were set to zero before averaging. The OE of 0.05 m/s for the current speed and 16° for direction were derived in agreement with measurement conditions and guidelines proposed by Van Rijn, Grasmeijer, and Ruessink (2000).

For data comparison, temporal and spatial coincidence of instantaneous measurements and model results was intended. However, because of the model outputs' resolution, there were temporal and spatial differences with the observed velocity profiles of up to 190 m and 5 minutes, respectively.

RESULTS

A quantitative evaluation of the model is considered in this section. The quantitative evaluation assessed the accuracy of the model in reproducing field observations through various statistical parameters. Later, the evaluated model was used to determine the flow patterns during the dry and rainy seasons. These patterns were qualitative compared to observations, as indicated in final sections.

Coupling Modeled and Field Data Obtained from Mobile Gauge Stations

The instantaneous adjustment between the observed and the modeled currents was statistically determined for the calibration and validation periods. Error classification and categorization of results according to the range of ARMAE values adopted by Sutherland *et al*. (2004) was used as reference to assess the hydrodynamic model accuracy. According to this method, an overall good performance of the model in the reproduction of the observed currents was obtained. Results are presented in Table 4.

The performance of the model when reproducing the observed currents in the transition period of November to December 2011 (additional validation test) was similar to that obtained previously during the dry and rainy seasons, ranging between reasonable to excellent. Some of these results are shown in Figure 4. This figure presents a comparison between measured and modeled values of the currents' speed and direction in the Gulf of Urabá. It includes data obtained in the transition, rainy, and dry seasons.

Table 3. *Value of the calibrated parameters of the hydrodynamic model.*

Parameter	Final Value	Range of Considered Values
Grid cells	21961	5490–43922
Depth layers	20	6–30
Layers 1–5, depth relative thickness (%)	2.5	
Layers 6–15, depth relative thickness (%)	5	
Layers 16–20, depth relative thickness (%)	7.5	
Time step (min)	1	0.1–4
Wind drag coefficient at 0 m/s	0.001	0.0006–0.003
Wind drag coefficient at 100 m/s	0.00723	
Manning roughness coefficient	0.02	0.015–0.03
Horizontal eddy viscosity (m^2/s)	500	1–500
Horizontal eddy diffusivity (m^2/s)	80	1–250
Vertical eddy viscosity	0.001*	0–0.001
Vertical eddy diffusivity	0*	0–0.005

* Values used as background (minimum) for the turbulent contribution calculated by the turbulence closure model (WL | Delft Hydraulics Staff, 2012).

Statistical assessment of the current discrepancies is indicated at the right-hand side of Figure 4. Pink and dark blue (in the top images) indicate currents heading north, while green corresponds to southward currents. In general, the ability of the model to reproduce the currents in the southern part of the gulf was reduced in comparison to central and northern areas; in addition, the model fails to reproduce an inverse circulation flow observed to the north of the main river inputs (more details in the Discussion section).

Coupling Modeled and Field Data Obtained from the Stationary Gauge Station

To complement the performance assessment of the model, an independent current dataset obtained from the upward-looking ADCP located near the NE boundary of the gulf was used. This dataset showed that surface currents tended to be strong, reaching maximum values up to 1.12 m/s and average values of 0.34 m/s. This current speed decreased gradually with depth, reaching maximum and mean bottom velocities of 0.56 and 0.1 m/s, respectively; the currents' predominant direction was NE (leaving the gulf) and it was substantially marked in the surface.

At this location, the model was able to reproduce fairly well the temporal variations of tides and waves. Discrepancies between observed and modeled tides and significant wave heights led to MAEs of 0.03 and 0.19 m, respectively. Predicted wave heights tended to follow the general behavior of the observed ones, and localized differences in the data might be caused by sudden wind variations not captured by the reanalysis projects. Unfortunately, there were no data from climatological stations to improve the wind forcing during this period.

The model was also capable to reproduce the one-layer outflow pattern observed in the NE area, where the gulf meets

Table 4. *Statistical assessment of the model performance (based on Sutherland* et al.*, 2004).*

Model Phase	Transect (Figure 2)	ARMAE Direction (magnitude)	Excellent <0.2	Good 0.2–0.4	Reasonable 0.4–0.7	Poor 0.7–1.0	Bad >1.0
Calibration	1	0.23 (0.58)		×	+		
	2	0.23 (0.54)		×	+		
	3	0.37 (0.29)		× +			
	4	0.57 (0.14)	+		×		
	5	0.31 (0.27)		× +			
Validation	6	0.36 (0.28)		× +			
	7	0.39 (0.37)		× +			
	8	0.12 (0.44)	×		+		
	9	0.46 (0.16)	+		×		
	10	0.53 (0.29)		+	×		

× is used for current direction; + is used for current speed.

the Caribbean Sea; however, it overestimates the eastern component of the currents. The coarse grid resolution (approximately 1 km) at the ADCP's mooring location affected the bathymetric representation and the model's accuracy (estimating the local currents) in this nearshore area. Figure 5 displays the adjustment between observed and modeled residual currents, tides, and waves. For compactness and better visualization of the semidiurnal tidal regime, tides are only displayed during a fortnight period.

Coupling Modeled and Field Data Obtained from CTD Profiles

Finally, an additional test to verify the performance of the model was carried out through the comparison of modeled and observed vertical profiles of temperature and salinity. A CTD profiler was deployed in 39 stations scattered throughout the gulf in November 2010 (Figure 6). Water salinity of about 35 or higher appeared mainly in the NW and below a 5- or 8-m depth. Brackish superficial waters cover the south (Bahia Colombia), central, and NE areas of the gulf.

Discrepancies between observed and modeled temperatures and salinities were determined through the MAE and RMAE statistical parameters. The MAE and RMAE of estimated temperatures were 0.4°C and 1.4%, respectively. Corresponding values for the estimated salinities were 1.5 and 4.6%. Figure 6 shows the observed and modeled profiles of salinity and temperature. The best adjustment was found in the north and central areas. Larger inaccuracies occurred in the southern and most protected area from wave action. Therefore, it is preliminary assumed that further steps considering the spatial variability of calibrated parameters (*i.e.* vertical eddy viscosity) might increase the performance of the model in both exposed and protected areas.

Flow Circulation Patterns

Two hydrodynamic simulations were carried out aiming to reproduce the currents during two representative climatic seasons. The two simulations were run during a 1-month period to compute flow variations within a tidal cycle and a tidal month. The external forces used for the rainy and dry seasons are shown in Table 5. Wind and wave characteristics correspond to the typical conditions for both seasons reported by Chevillot *et al*. (1993).

Tides (defined in Table 5), solar radiation, and atmospheric pressure (obtained from the NCEP/NCAR reanalysis project) were considered time dependent, while the remaining forces were kept constant during the simulations (Table 5). This removed most of the short-term fluctuations that occur as a consequence of the stochastic nature of atmospheric conditions. In this case, temporal variations of the currents were mainly generated by tides.

Synoptic observations of the model results for the surface and bottom layers allowed a graphical representation of the spatial and temporal variations of the marine currents. In Figure 7, the streamlines show the typical flow directions computed within the simulation periods. Bights located in the narrower area of the gulf present distinctive flood and ebb currents (because of increased relevance of tides). This condition is represented with arrows on both ends of the streamlines. Current speed variations within neap and spring tidal cycles (in the a–h locations, defined in the top-left image) are shown with color bars. The same figure also displays the areas most affected by wave processes. The latter is indicated by means of background colors expressing wave-induced forces (time averaged) and maximum bed shear stresses for the combined action of waves and currents.

The top- and bottom-left illustrations from Figure 7 represent the characteristic flow during the rainy season, in which the wind and waves were moderate. In this season, the surface currents (low-brackish salinities) were principally directed toward the north (leaving the gulf). As depth increased, the flow in the southern direction gradually became relevant, especially to the north of the Leoncito mouth. This two-layer pattern can be altered in some areas because of (1) the lateral discharge of the Atrato River, which generates a three-layer pattern in Bahia Colombia; (2) the spring tide in flood phases, creating a one-layer inflow in the narrower area of the gulf; and (3) the interaction with the Caribbean Sea, where a one-layer outflow in the NE boundary dominates the dynamics. Finally, in nearshore areas, fluctuations of the currents resulted because of the stirring of waves.

During the simulation of the dry season, stronger trade winds and higher waves both coming from the NE were considered. The increase in wind speed and drag forces drove surface currents typically leaving the gulf in the opposite direction, in a way similar to that observed in other regions with freshwater influence (Simpson, 1997). Deeper currents kept their southern direction. As the water flowed into the gulf through the surface and bottom layers, the outflow appeared at an intermediate layer (Figure 8).

In general, the surface currents tended to be greater than those in the intermediate and bottom layers. The greatest velocities were predicted close to the Atrato's main distribu-

Table 5. *External forcings used in the hydrodynamic model to determine flow circulation patterns.*

	Dry Season	Rainy Season	Extreme Event
Forces Range			
Wind speed (m/s)	8	3	12
Wind direction (°)	30	180	30
Significant wave height (m)*	1.5	0.75	3.5
Wave direction (°)*	30	0	30
Wave period (s)*	6.2	5	11
Discharge of the Atrato River (m^3/s)	4138	5017	4138
NW salinity S (B)†	27 (30)	34.5 (36)	27 (30)
NE salinity S (B)†	20.2 (22.1)	33.5 (36)	20.2 (22.1)
NW temperature (°C) S (B)†	28.8 (28)	28.4 (28.6)	28.8 (28)
NE temperature (°C) S (B)†	28.8 (28.4)	28.3 (28.7)	28.8 (28.4)
Tidal Components [amplitude (m)/phase (°)]			
M2 0.0692/151.94			
N2 0.0254/121.05			
K1 0.0935/239.33			
O1 0.0575/240.17			
P1 0.0290/244.30			
Q1 0.0082/235.86			
MF 0.0168/356.52			
MM 0.0081/353.33			
M4 0.0019/151.68			
MS4 0.0050/340.23			
MN4 0.0018/193.10			

* These values correspond to the incoming swell from the Caribbean boundary.
† Model input of salinity and temperature along the northern boundary was based on CTD profiles carried out at the 4 stations presented in Figure 1 for the two climatic seasons.
S denotes surface; B denotes bottom.

taries (El Roto, Matuntugo, and Leoncito), with values up to 1.2 m/s; significant velocity values also resulted on the NE shore near Punta Caribaná. Current variation during a tidal cycle was relatively low, as indicated in the plots of Figure 7. An exception to this statement occurred in the narrower zone of the gulf (the g location). In this area, the currents were substantially reinforced or weakened during spring tides.

The tidally averaged flow in the gulf was defined through the model results after the integration of the currents in longitudinal (AB) and transverse (CD) sections (Figure 3) during a 14.7-day period. Figure 8 displays the model results of the two characteristic climatic seasons and those of a simulation in which the wave and wind forces were considerably increased to resemble an extreme weather event, with external forcings determined in agreement with the values proposed by Osorio *et al*. (2010) and Chevillot *et al*. (1993), as shown in Table 5.

The stability of the stratification in section CD was determined by means of the Richardson number (Ri). A critical value of 0.25 was adopted (Miles, 1987; Richardson, 1920) to separate areas with higher mixing ($Ri < 0.25$) from those with stable stratification ($Ri > 0.25$). The computed variation of the Ri across section CD showed the enhancement of mixing processes in a surface layer of about 4 m during the dry season, indicating the effect of stronger winds and waves. The unstable region in the bottom layer became larger in the narrower zone of the gulf, which might be associated to stronger tidal currents.

The tidally averaged currents confirm the different circulation patterns during the rainy and dry seasons. The rainy season presented a two-layer flow, while in the dry season a three-layer structure with middle outflow and surface–bottom inflow was computed. This three-layer structure (left column of Figure 8) seemed to persist in Bahia Colombia even during the

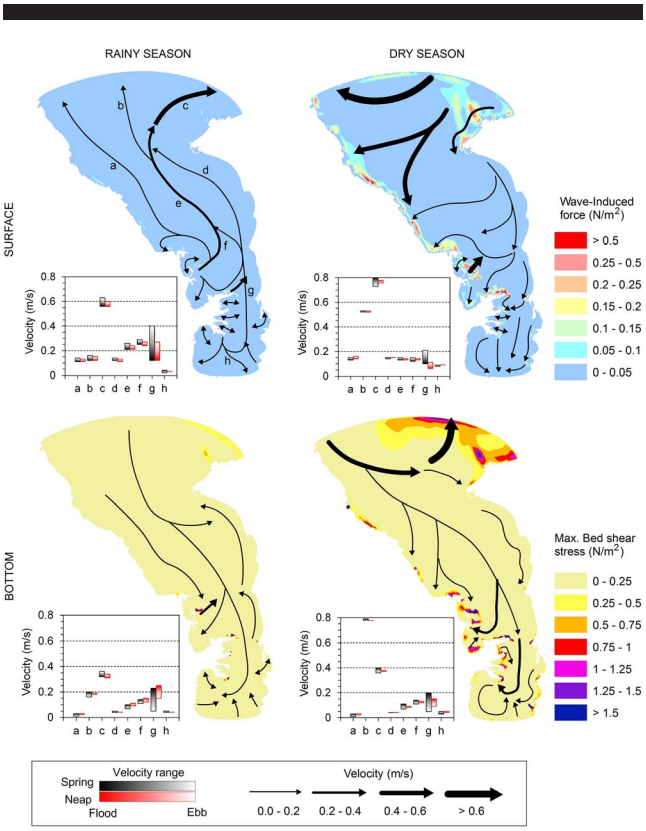

Figure 7. Modeled circulation patterns and spatial distribution of (top) wave-induced forces and (bottom) bed shear stresses in the Gulf of Urabá. (Color for this figure is available in the online version of this paper.)

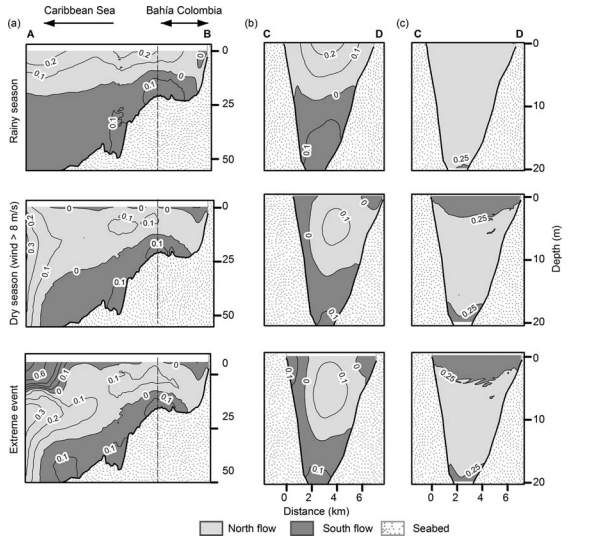

Figure 8. Vertical view of the flow circulation in the Gulf of Urabá. (A) Tidally averaged velocity (in meters per second) along section AB. (B) Tidally averaged velocity (in meters per second) across section CD. (C) Ri in section CD.

rainy season. In the extreme event, the three-layer structure occurred and tended to shift into a two-layer flow. However, flow directions were opposite those indicated during the rainy season.

DISCUSSION

A proper combination of current data from mobile (spatial flow variations) and stationary (temporal flow variations) gauge stations would be ideal for development of estuarine flow models. Measurements from mobile stations should be carried out as a first stage to initially identify the location of probable flow patterns; then, detailed confirmation of these patterns could be done through numerical modeling and stationary stations strategically located accordingly to the findings of the initial phase of data collection.

Consequently, to verify whether observed instantaneous currents (from a mobile gauge station) correspond to a pattern, the following conditions should be considered: (1) independent measuring campaigns carried out during different periods of the year show similar instantaneous flows in the same area (Figure 9), (2) the numerical model can reproduce the observed instantaneous flow and confirms that over time it tends to be persistent, and (3) measurements from a stationary gauge station confirm the existence of the pattern.

Based on previous indications, various flow patterns were identified in the gulf. First, two-layer typical estuarine circulation (Pritchard, 1955; Dyer, 1997) was noted in the gulf's central part. The river plume leaves the gulf on the surface and heads toward the Caribbean Sea. As depth increases, salty water enters the gulf. Both the model (Figures 4 and 8) and the observations in the three measuring campaigns (Figure 9) confirm the existence of this pattern.

Second, a three-layer flow pattern was observed in Bahia Colombia (south of the gulf). The surface and bottom layers of water are driven southward, while the water in the intermediate layer is moving northward. Then, surface currents are opposite to those typically observed in estuaries. The model was able to reproduce this pattern (Figure 8, section AB), which was also observed in the field (Figure 9). This pattern is probably because of the lateral freshwater discharge of the Atrato River into the gulf, which tends to spread radially from its source and generate both north (seaward) and south (inland) surface buoyant currents. The south-oriented mouth of the Leoncito distributary in Bahia Colombia reinforces these southward currents. A similar circumstance has been also observed in other regions of freshwater influence (Montoya, 2010; O'Donnell, 1990; Simpson, 1997).

Third, a one-layer outflow was found at the NE boundary of the gulf. Between Necoclí and Punta Caribaná, the typical estuarine flow is again modified; the surface outflow becomes thicker and extends along the water column, forming a one-layer pattern that delivers the water of the gulf into the Caribbean Sea. The model could reproduce this pattern (top-left illustration from Figure 5), which was observed using the mobile (Figure 9) and the stationary (Figure 5) gauge stations.

The earth-rotation effect (even in this tropical region) might contribute to or cause the outflow to lean toward the right (looking seaward), as has been shown in the Northern Hemisphere by Garvine (1987) and O'Donnell (1990). Montoya (2010) determined a Rossby number lower than 1 in this area of the gulf and stated the relevance of the Coriolis force in the flow circulation.

Some observed and modeled flows could be also part of the circulation pattern in the gulf, although future work should confirm them. First, under strong northerly winds (*i.e.* in the dry season), the typical estuarine circulation is modified to three layers, where inflow (south direction) occurred in the surface (because of wind drag) and bottom layers and outflow appeared in an intermediate layer. Measurements carried out during the dry season (April 2010) took place under relative calm weather, limiting the possibility to confirm this modeled circulation pattern. Montoya (2010) predicted this flow, because he found a comparable strength between advective and wind processes. This was based on the similar value of the Rossby and Eckman transport numbers. Therefore, if wind and advection were opposite (usually occurring in the dry season), seaward-surface currents could be blocked and even turned landward.

Second, a three-layer flow and inverse circulation occurred to the north of main river inputs. The surface and bottom water is driven seaward, and the water in the intermediate layer is driven landward. This pattern, indicated in Figure 9, was not reproduced by the model. Because this pattern was observed further north from the main distributaries of the Atrato River and under an extreme rainy period, the possibility of a hyperpycnal flow occurrence is considered. Against this idea, suspended sediment concentrations of the river were always below 1 kg/m^3. Nevertheless, some other factors can increase the possibility of hyperpycnal flow formation under lower river

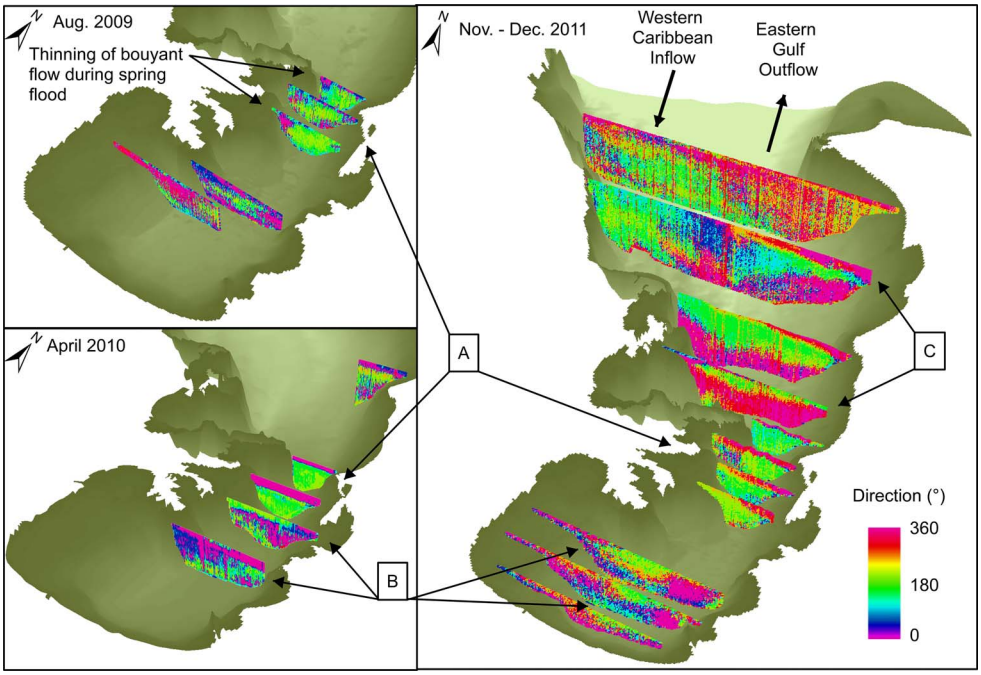

Figure 9. Circulation patterns in the Gulf of Urabá based on observed current direction. (A) Typical estuarine circulation. (B) Three-layer pattern in Bahia Colombia. (C) Inverse circulation. (Color for this figure is available in the online version of this paper.)

sediment concentrations (Mulder *et al*., 2003), such as the soft and easily erodible deposits of the Atrato River delta and the possible occurrence of convective instability. Additional information is required to precisely define the nature of this bottom flow heading north.

Tidal effect on the current speed and direction was quite low in the entire study area. However, the exception occurred in the narrower zone of the gulf between the mouths of the Leoncito and Matuntugo distributaries of the Atrato River. In this area, tides became more relevant and could even reverse buoyant currents during spring flood phases. Wave-driven currents were more conspicuous during the dry season. The areas most affected by wave processes corresponded to the shallower NW zone, river deltas, and Punta Caribaná and, with less intensity, along the eastern coast (Figure 7). However, the directional variation of the waves approaching the gulf, from NE to NW, leads to higher wave-induced forces along the east coast, especially between the Turbo and the Necoclí municipalities. This situation, in combination with poor lithological conditions (Correa and Vernette, 2004), can explain, to a certain extent, existing problems of coastal erosion.

Absence of a systematic program to measure oceanographic, climatic, and limnigraphic data in the region obliged the use of alternative data sources to determine some of the external forcings of the model. Their coarse resolution or less accuracy near the coast could affect the performance of the model, especially in the reproduction of scenarios implying high temporal or spatial variations of the marine dynamics.

CONCLUSIONS

A 3D hydrodynamic model of the Gulf of Urabá was evaluated with good performance using quantitative and qualitative approaches. The quantitative validation was achieved under a demanding and unusual process using instantaneous data of vertical velocity profiles. These profiles were obtained along transects spread over the gulf in three seasons. This type of data was preferred instead of that obtained from stationary stations, though at the expense of short-term temporal resolution.

Model results and measurements under calm weather conditions showed complex water circulation in the gulf formed by various flow patterns. These patterns correspond with several mechanisms that become dominant in certain regions or seasons. A two-layer typical estuarine circulation revealed the importance of baroclinic forcings in the central part of the gulf. Atrato River's advection and wind forcing can turn this estuarine circulation into a three-layer flow in Bahia Colombia and even in a larger area during the dry season. A one-layer outflow pattern occurs in the NE area of the gulf, similar to those induced by a Coriolis force in higher latitudes.

Tide and wave forcings also affect currents in the gulf. However, their relevance was more restricted in space and time. Tides and associated barotropic flows become notable in the narrower area of the gulf, especially during spring tides. However, wave-induced currents become relevant in nearshore areas (except Bahia Colombia) during dry seasons. Finally, an inverse circulation flow to the north of main distributaries of the Atrato River (Matuntugo and Roto) takes place, completing the marine currents in the gulf.

ACKNOWLEDGMENTS

Field data and mathematical models used in this study were obtained from the research projects "Erosión Costera en Antioquia: Dinámica sedimentaria del Golfo de Urabá (erosión-depositación) durante los ultimos 10,000 años" and "Erosión Costera en Antioquia II: Modelación de la evolución morfológica en el Golfo de Urabá." The authors thank the Departamento de Ciencia, Tecnología e Innovación; Universidad Escuela de Administración, Finanzas y Tecnología EAFIT; Universidad de Antioquia; Universidad Nacional; and the Centro de Investigaciones Oceanográficas e Hidrográficas del Caribe for funding these projects. The authors also thank the port authorities of Turbo for logistical support provided during the field campaigns.

LITERATURE CITED

BIRD (Banco de Iniciativas Regionales para el Desarrollo de Antioquia), 2010. *Iniciativas de Conexión de Antioquia con el Noroccidente Colombiano*. Medellín, Colombia: BIRD, 193p.

Booij, N.; Ris, R.C., and Holthuijsen, L.H., 1999. A third generation wave model for coastal regions. Part I: Model description and validation. *Journal of Geophysical Research,* 104(C4), 7649–7666.

Chevillot, P.; Molina, A.; Giraldo, L., and Molina, C., 1993. Estudio geológico e hidrológico del Golfo de Urabá. *Boletín Científico CIOH,* 14, 79–89.

Correa, I.D. and Vernette, G., 2004. Introducción al problema de la erosión litoral en Urabá (sector Arboletes-Turbo) Costa Caribe Colombiana. *Boletín de Investigaciones Marinas y Costeras (INVEMAR),* 33, 7–28.

Díaz, J.M., 2007. *Deltas y Estuarios de Colombia*. Cali, Colombia: Banco de Occidente, 208p.

Díaz, J.M.; Díaz, G., and Sánchez, J.A., 2000. Distribution and structure of the southernmost Caribbean coral reefs: Golfo de Urabá, Colombia. *Scientia Marina,* 64(3), 327–336.

Dingemans, M.W.; Radder, A.C., and de Vriend, H.J., 1987. Computation of the driving forces of wave-induced currents. *Coastal Engineering,* 11(247), 539–563.

Dyer, K., 1997. *Estuaries. A Physical Introduction*. Chichester, U.K.: Wiley Interscience, 195p.

Egbert, G.D. and Erofeeva, L., 2002. Efficient inverse modeling of barotropic ocean tides. *Journal of Atmospheric and Oceanic Technology,* 19, 183–204.

Escobar, C.A., 2011. Relevancia de los procesos costeros en la hidrodinámica del Golfo de Urabá (Caribe Colombiano). *Boletín de Investigaciones Marinas y Costeras,* 40(2), 101–120.

Fredsöe, J., 1984. Turbulent boundary layer in wave–current interaction. *Journal of Hydraulic Engineering,* 110(71), 1103–1120.

Fredsöe, J. and Deigaard, R., 1992. *Mechanics of Coastal Sediment Transport*. Singapore: World Scientific Publishing, 369p.

García, C., 2007. *Atlas del Golfo de Urabá: Una Mirada al Caribe de Antioquia y Chocó*. Santa Marta, Colombia: Instituto de Investigaciones Marinas y Costeras–Invemar and Gobernación de Antioquia, 180p.

Garvine, R., 1987. Estuary plumes and fronts in shelf waters: A layer model. *Journal of Physical Oceanography,* 17, 1877–1896.

Gerritsen, H.; De Goede, E.D.; Platzek, F.W.; Genseberger, M.; Van Kester, J.A.Th.M., and Uittenbogaard, R.E., 2007. Validation Document Delft3D-FLOW: A Software System for 3D Flow Simulations. *Report X0356, M3470*. Delft, The Netherlands: WL | Delft Hydraulics, 266p.

Hastenrath, S., 1990. Diagnostics and prediction of anomalous river discharge in the northern South America. *Journal of Climate,* 3, 1080–1096.

Henao, H. and Correa, G., 2007. Conexión férrea interoceánica una ruta dos mares: Canal seco interoceánico. *Proceedings of the 1st Integrated National Symposium of Transport and Roads* (Bogotá, Colombia), Paper 11, 23p.

Hubach, E., 1930. Apreciación de los proyectos de canal interoceánico por el Napipí y el Truandó según puntos de vista geológicos. *Boletín de Minas y Petróleo,* 13, 15–34.

Kalnay, E.; Kanamitsu, M.; Kistler, R.; Collins, W.; Deaven, D.; Gandin, L.; Iredell, M.; Saha, S.; White, G.; Woollen, J.; Zhu, Y.; Leetmaa, A.; Reynolds, R.; Chelliah, M.; Ebisuzaki, W.; Higgins, W.; Janowiak, J.; Mo, K.C.; Ropelewski, C.; Wang, J.; Jenne, R., and Joseph, D., 1996. The NCEP/NCAR 40-year reanalysis project. *Bulletin of the American Meteorological Society,* 77(3), 437–471.

Leendertse, J.J., 1967. *Aspects of a Computational Model for Long-Period Water–Wave Propagation*. Santa Monica, California: Rand Corporation, *Memorandum RM-5294-PR*, 165p.

Lesser, G.R.; Roelvink, J.A.; Van Kester, J.A.T.M., and Stelling, G.S., 2004. Development and validation of a three-dimensional morphological model. *Coastal Engineering,* 51(8–9), 883–915.

Lonin, S. and Vasquez, J.G., 2005. Hidrodinámica y distribución de coliformes en el Golfo de Urabá. *Boletín Científico CIOH,* 23, 76–89.

Melman, F., 2011. Navigability at an Unstable Bifurcation: The Montaño–Murindó Bifurcation of the Atrato River in Colombia. Delft, The Netherlands: Delft University of Technology, Master's thesis, 127p.

Mesinger, F.; Dimego, G.; Kalnay, E.; Mitchell, K.; Shafran, P.C.; Ebisuzaki, W.; Jovic, D.; Woollen, J.; Rogers, E.; Berbery, E.H.; Ek, M.B.; Fan, Y.; Grumbine, R.; Higgins, W.; Li, H.; Lin, Y.; Manikin, G.; Parrish, D., and Shi, W., 2006. North American regional reanalysis. *Bulletin of the American Meteorological Society,* 87(3), 343–360.

Miles, J., 1987. Richardson's number revisited. *Proceedings of the 3rd International Symposium of Stratified Flows* (Pasadena, California), pp. 1–7.

Molina, A.; Molina, C., and Chevillot, P., 1992. La percepción remota aplicada para determinar la circulación de las aguas superficiales del Golfo de Urabá y las variaciones de su linea de costa. *Boletín Científico CIOH,* 11, 43–58.

Montoya, L.J., 2010. Dinámica Oceanográfica del Golfo de Urabá y su Relación con los Patrones de Dispersión de Contaminantes y Sedimentos. Medellín, Colombia: Universidad Nacional de Colombia, Ph.D. thesis, 254p.

Mulder, T.; Syvitski, J.P.M.; Migeon, S.; Faugeres, J., and Savoye, B., 2003. Marine hyperpycnal flows: Initiation, behavior and related deposits—A review. *Marine and Petroleum Geology,* 20, 861–882.

Octavio, K.A.H.; Jirka, G.H., and Harleman, D.R.F., 1977. *Vertical Heat Transport Mechanisms in Lakes and Reservoirs*. Cambridge, Massachusetts: Massachusetts Institute of Technology, *Technical Report 227*, 131p.

O'Donnell, J., 1990. The formation and fate of a river plume: A numerical model. *Journal of Physical Oceanography,* 20, 551–568.

Osorio, A.; Gómez, A.; Molina, L.; Álvarez, O., and Osorio, J., 2010. Bases metodológicas para caracterizar el oleaje local (sea) y de fondo (swell) en el Golfo de Urabá. *Proceedings of the 24th Congreso Latinoamericano de Hidráulica* (Punta del Este, Uruguay, AIIH), 12p.

Phillips, N.A., 1957. A co-ordinate system having some special advantages for numerical forecasting. *Journal of Meteorology,* 199(14), 184–185.

Post, S., 2011. Morphological Modelling of the Atrato River Delta in Colombia. Delft, The Netherlands: Delft University of Technology, Master's thesis, 147p.

Poveda, G. and Mesa, O.J., 1997. Feedbacks between hydrological processes in tropical South American and large-scale ocean–atmospheric phenomenon. *Journal of Climate,* 10, 2690–2702.

Pritchard, D.W., 1955. Estuarine circulation patterns. *Proceedings of the American Society of Civil Engineers,* 81(717), 1–11.

Richardson, L.F., 1920. The supply of energy from and to atmospheric eddies. *Proceedings of the Royal Society of London A,* 97, 354–373.

Rodi, W., 1980. *Turbulence Models and Their Application in Hydraulics—A state-of-the-art review*. Delft, The Netherlands: International Association for Hydraulics Research, 124p.

Roelvink, J.A. and Van Banning, G.K.F.M., 1994. Design and development of Delft3D and application to coastal morphodynamics. *In:* Verwey, A.; Minns, A.W.; Babovic, V., and Maksimovic, C. (eds.), *Hydroinformatics '94: Proceedings of the 1st International*

Conference on Hydroinformatics (Delft, The Netherlands), pp. 451–455.

Roldán, P.A., 2008. Modelamiento del Patrón de Circulación de la Bahía Colombia, Golfo de Urabá. Medellín, Colombia: Universidad Nacional de Colombia, Master's thesis, 109p.

Saltelli, A.; Tarantola, S., and Campolongo, F., 2000. Sensitivity analysis as an ingredient of modelling. *Statistical Science,* 15(4), 377–395.

Simpson, J., 1997. Physical processes in the ROFI regime. *Journal of Marine Systems,* 12, 3–15.

Stelling, G.S. and Leendertse, J.J., 1991. Approximation of convective processes by ciclyc AOI methods. *Proceedings of the 2nd International Conference on Estuarine and Coastal Modelling* (New York, ASCE), pp. 771–782.

Sutherland, J.; Walstra, D.J.R.; Chesher, T.J.; Van Rijn, L.C., and Southgate, H.N., 2004. Evaluation of coastal area modelling systems at an estuary mouth. *Coastal Engineering,* 51, 119–142.

Tolman, H.L., 1989. *The Numerical Model WAVEWATCH: A Third Generation Model for Hindcasting of Wind Waves on Tides in Shelf Seas*. Delft, The Netherlands: Delft University of Technology, *Technical Report 892*, 72p.

Trautwine, J.C., 1854. Rough notes of an exploration for an interoceanic canal route by way of the Rivers Atrato and San Juan, in New Granada, South America. *Journal of the Franklin Institute,* 54(4), 96p.

Van Rijn, L.C.; Grasmeijer, B.T., and Ruessink, B.G., 2000. *Measurements Errors of Instruments for Velocity, Wave Height, Sand Concentration and Bed Level in Field Conditions*. Delft, The Netherlands: WL | Delft Hydraulics, 47p.

Velasquez, L., 2013. Modelación del Transporte de Sedimentos en el Golfo de Urabá, Colombia. Medellín, Colombia: Universidad EAFIT, Master's thesis, 132p.

Velez, J.; Poveda, G., and Mesa, O., 2000. *Balances Hidrológicos de Colombia*. Medellín, Colombia: Universidad Nacional de Colombia, 150p.

Walstra, D.J.R. and Roelvink, J.A., 2000. 3D calculation of wave driven cross-shore currents. *Proceedings of the 27th International Conference on Coastal Engineering* (Sydney, Australia), pp. 1050–1063.

WL | Delft Hydraulics Staff, 2012. *Delft3D-Flow. Simulation of Multi-Dimensional Hydrodynamic Flows and Transport Phenomena, Including Sediments. User Manual Version 3.15.25157*. Delft, The Netherlands: Deltares, 630p.